Homoclinic and heteroclinic chaos in nonlinear systems driven by trichotomous noise*

You-Ming Lei(雷佑铭) and Hong-Xia Zhang(张红霞)†

Department of Applied Mathematics, Northwestern Polytechnical University, Xi'an 710072, *China*

(Received 28 October 2016; revised manuscript received 15 December 2016; published online 13 February 2017)

The homoclinic and heteroclinic chaos in nonlinear systems subjected to trichotomous noise excitation are studied. The Duffing system and the Josephson-junction system are taken for example to calculate the corresponding amplitude thresholds for the onset of chaos on the basis of the stochastic Melnikov process with the mean-square criterion. It is shown that the amplitude threshold for the onset of chaos can be adjusted by changing the internal parameters of trichotomous noise, thereby inducing or suppressing chaotic behaviors in the two systems driven by trichotomous noise. The effects of trichotomous noise on the systems are verified by vanishing the mean largest Lyapunov exponent and demonstrated by phase diagrams and time histories.

Keywords: trichotomous noise, chaos, Melnikov method, Lyapunov exponent

PACS: 05.45.−a, 05.45.Pq, 02.50.Ey **DOI:** 10.1088/1674-1056/26/3/030502

1. Introduction

The chaotic motion is a kind of irregular and random movement due to sensitive dependence on initial conditions, and it has been studied by many methods such as the largest Lyapunov exponent, Poincare map, power spectrum, fractal dimension, and Melnikov method. Outstanding among them is the Melnikov technique, which renders an analytical method available for the detection of chaotic motions. It was used by Koch and Leven[1] to identify boundaries of subharmonic and homoclinic bifurcations depending on the parameters of a forced pendulum system. With this method, Ariaratnam *et al.*[2] discussed homoclinic chaos prediction subjected to an axial excitation for the transverse vibration of a buckled column. Shaw and Rand[3] studied the chaotic motions in an inverted pendulum with rigid barriers subjected to periodic excitations. Xie[4] modified the Melnikov method and used it to explore the effect of Gaussian white noise excitation on the chaotic motion of a buckled column. Further, Lin and Yim[5] defined a stochastic Melnikov process and developed the stochastic Melnikov method of determining the threshold for noisy chaos. They observed that external noise has significant effect on the transition from noisy periodic attractor to chaos. Awrejcewicz *et al.*[6–8] predicted the existence of chaos in a four-dimensional self-excited system and a class of lumped mechanical system with Coulomb-like friction and dry friction, respectively. The stochastic Melnikov technique was applied by Lei[9] to an averaged oscillator in order to determine the threshold of random excitation amplitude for the onset of chaos. Zhang *et al.*[10] utilized an extended Melnikov method to investigate the multi-pulse global bifurcations and chaotic dynamics of the nonlinear cantilever beam oscillations driven by harmonic axial transverse excitations at the free end in the resonant case. The Melnikov method was also employed by Yang *et al.*[11] to obtain the chaotic threshold for a nonlinear system under the perturbation of external forcing.

Trichotomous noise, a particular case of non-Gaussian colored noise,[12] can be regarded as a stochastic telegraph process like dichotomous noise, whose effect on dynamic systems has been analyzed by many researchers.[13–18] However, trichotomous noise can represent real noise better than dichotomous noise in actual applications because the former can degenerate into the latter and is more flexible to model random fluctuations in nature.[19] Besides, trichotomous noise can be directly expressed as a physical condition such as the heat transfer between three states or configurations. It has been developed to mimic the fluctuations of the oscillator frequency and mass.[20–23] The influence of variable environment on the population carrying capacity was also modified as the colored three-level Markovian noise.[24] Most of the past research on trichotomous noise focused on the cases of stochastic resonance. For example, Mankin *et al.* investigated trichotomous-noise-induced transitions[20] and explored the stochastic resonance phenomenon in some linear systems subjected to trichotomous noise.[25–27] The cases of stochastic resonance of a linear oscillator with random damping parameter,[28] several fractional oscillators,[29–31] the coupled underdamped bistable systems[32] and the FitzHugh–Nagumo neuron model[33] driven by trichotomous noise have also been

*Project supported by the National Natural Science Foundation of China (Grant No. 11672231), the Natural Science Foundation of Shaanxi Province, China (Grant No. 2016JM1010), the Fundamental Research Funds for the Central Universities, China (Grant No. 3102015ZY073), and the Seed Foundation of Innovation and Creation for Graduate Students in Northwestern Polytechnical University, China.

†Corresponding author. E-mail: zhanghongxia@mail.nwpu.edu.cn

© 2017 Chinese Physical Society and IOP Publishing Ltd

analyzed. Zhong *et al.*[30] studied two different forms of the generalized stochastic resonance phenomena versus trichotomous noise intensity. For the stochastic chaos, several studies have focused on systems induced by Gaussian noise[34,35] or Poisson noise.[36,37] Lei *et al.*[17] studied the chaos in a generalized Duffing-type oscillator with a fractional-order deflection subjected to dichotomous noise excitation. They showed that for such an oscillator, the threshold of chaos can be enhanced and then chaotic behaviors can be controlled while appropriately changing the transition rate of dichotomous noise. However, chaos in the system driven by trichotomous noise has not been studied so far.

In this study, the effects of trichotomous noise on chaos in the Duffing system[38–41] and the Josephson-junction system[42–44] are discussed, respectively, with the stochastic Melnikov method. The rest of the paper is organized as follows. Trichotomous noise is generated numerically, and then its spectral density is derived and depicted in Section 2. In Section 3 the necessary condition for the appearance of chaos is discussed based on the two illustrative systems by the stochastic Melnikov method with the mean-square criterion. In Section 4, the analytical results including the mean largest Lyapunov exponent, phase diagrams and time histories are verified by numerical methods. Finally, conclusions are drawn in Section 5.

2. Trichotomous noise

2.1. Generation of trichotomous noise

One can extend the notion of dichotomous noise further to trichotomous noise denoted by $\xi(t)$ which is a stationary Markovian process. The process is composed of jumps between three values a, 0 and $-a$, while the values rise with the respective stationary probabilities

$$P_{\rm s}(a) = P_{\rm s}(-a) = q, \;\; P_{\rm s}(0) = 1-2q. \tag{1}$$

The transition probabilities[20] between three states $\xi(t) = \pm a$ and 0 are obtained as

$$\begin{aligned} &P(\pm a, t+\Delta t|0,t) = P(\pm a, t+\Delta t|\mp a, t) = q(1-{\rm e}^{-\nu\Delta t}),\\ &P(0, t+\Delta t|\pm a, t) = (1-2q)(1-{\rm e}^{-\nu\Delta t}),\\ &\Delta t > 0,\ 0 < q < 0.5,\ \nu > 0, \end{aligned} \tag{2}$$

where ν is the switching rate that is related to noise correlation time τ by

$$\nu = 1/\tau. \tag{3}$$

The generation of trichotomous noise is completely determined by Eqs. (1) and (2).

Figures 1(a)–1(c) present the generation of trichotomous noise for the values $1, 0, -1$ as a time-dependent function for different values of correlation time τ and probability q numerically. It is clear to observe that as the correlation time τ increases, residence time grows or jump frequency shrinks at the three values from Figs. 1(a)–1(b), which means that the randomness is weakened. Furthermore, it is also worth noting that trichotomous noise can approach dichotomous noise which only jumps between two values 1 and -1 in the case $q = 0.5$ shown in Fig. 1(c), which explains dichotomous noise as a special case of trichotomous noise.

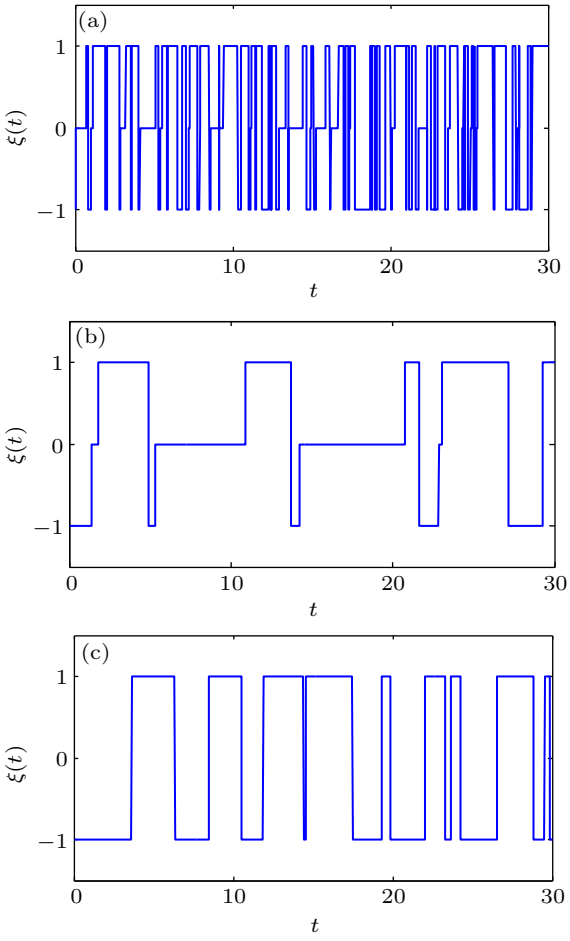


Fig. 1. (color online) Generation of trichotomous noise for the values $1, 0, -1$, for different values of parameter: (a) $q = 0.3, \tau = 0.1$; (b) $q = 0.3, \tau = 1$; (c) $q = 0.5, \tau = 1$.

2.2. Spectral density of trichotomous noise

We calculate the mean value

$$\langle \xi(t) \rangle = \sum_{x=-a,0,a} x P_{\rm s}(x) = 0, \tag{4}$$

and the correlation function

$$\begin{aligned} \langle \xi(t)\, \xi(t') \rangle &= \sum_{xx'} xx' P(x,t|x',t') P_{\rm s}(x')\\ &= \sum_{x'} x' P_{\rm s}(x') \sum_{x} x P(x,t|x',t')\\ &= 2qa^2\, {\rm e}^{-\nu|t-t'|}. \end{aligned} \tag{5}$$

Then the spectral density of trichotomous noise $\xi(t)$, as the Fourier transform of the correlation function, can be obtained as

$$S(\omega) = 2qa^2\nu/\pi\left(\omega^2+\nu^2\right). \tag{6}$$

Here, we fix $a=1$ to show the spectral density of trichotomous noise for several values of parameters τ, q in Fig. 2. It is obvious that the spectral density is always symmetrical about the straight line $\omega=0$ which is also the position of the spectral density peak. From Fig. 2(a), we observe that when q is fixed at 0.3, the bigger the value of τ, the larger the peak value of the spectral density is, and at the same time the narrower the bandwidth of the one is, implying the less the randomness of the noise is. While τ is fixed at 1, the larger the value of q, the larger the peak value of the spectral density is, as shown in Fig. 2(b). These illustrate that the parameters correlation time τ and probability q have effects on the spectral density of trichotomous noise to different extents.

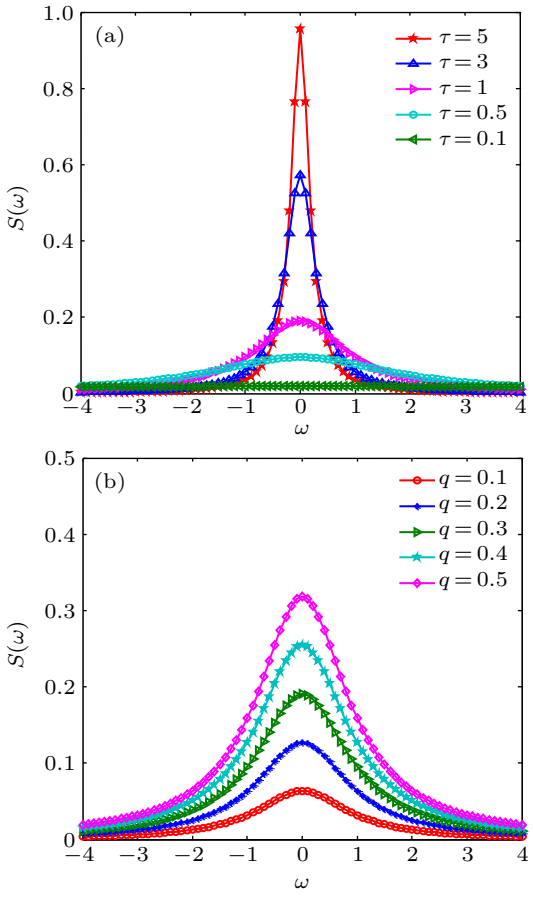


Fig. 2. (color online) Spectral densities of trichotomous noise for different values of parameter: (a) $q=0.3$ and (b) $\tau=1$.

3. Stochastic Melnikov method

3.1. Chaos threshold with the stochastic Melnikov method

The Melnikov method, developed by Wiggins,[45] of measuring the distance between stable and unstable manifolds, is aimed at predicting whether chaos occurs.

Consider the two-dimensional perturbed Hamiltonian system as follows:

$$\begin{aligned}\dot{x} &= \frac{\partial H(x,y)}{\partial y}+\varepsilon g_1(x,y,t),\\ \dot{y} &= -\frac{\partial H(x,y)}{\partial x}+\varepsilon(g_2(x,y,t)+\mu\xi(t)),\end{aligned} \tag{7}$$

where $0<\varepsilon\ll 1$ denotes a perturbative parameter, $H(x,y)$ represents the Hamiltonian function of the unperturbed system, and μ is the amplitude representing the intensity of trichotomous noise $\xi(t)$. For simplicity, system (7) can be rewritten as the following vector form:

$$\dot{\boldsymbol{X}} = \boldsymbol{F}(\boldsymbol{X})+\varepsilon\boldsymbol{G}(\boldsymbol{X},t), \tag{8}$$

where

$$\begin{aligned}\boldsymbol{F}(\boldsymbol{X}) &= \left(\frac{\partial H}{\partial y},-\frac{\partial H}{\partial x}\right)^{\mathrm{T}},\\ \boldsymbol{G}(\boldsymbol{X},t) &= (g_1(x,y,t),g_2(x,y,t)+\mu\xi(t))^{\mathrm{T}}.\end{aligned}$$

When $\varepsilon=0$, the corresponding unperturbed system is

$$\dot{\boldsymbol{X}} = \boldsymbol{F}(\boldsymbol{X}). \tag{9}$$

If system (9) has a homoclinic or heteroclinic orbit $\boldsymbol{\Gamma}(t)=(x(t),y(t))^{\mathrm{T}}$, then the Melnikov process of the orbit can be obtained as

$$\begin{aligned}M(t_0) &= \int_{-\infty}^{+\infty}\boldsymbol{F}(\Gamma(t))\boldsymbol{\Lambda}\boldsymbol{G}(\Gamma(t),t+t_0)\,\mathrm{d}t\\ &= \int_{-\infty}^{+\infty}\left(\frac{\partial H(x,y)}{\partial y}(g_2(x,y,t+t_0)+\mu\xi(t+t_0))\right.\\ &\quad\left.+\frac{\partial H(x,y)}{\partial x}g_1(x,y,t+t_0)\right)\Big|_{\boldsymbol{\Gamma}(t)}\mathrm{d}t\\ &= M_{\mathrm{d}}+\mu M_{\mathrm{s}},\end{aligned} \tag{10}$$

where $\boldsymbol{\Lambda}$ is the projection operator. For example, if $\boldsymbol{a}=(a_1,a_2)^{\mathrm{T}}$ and $\boldsymbol{b}=(b_1,b_2)^{\mathrm{T}}$, then

$$\boldsymbol{a}\,\Lambda\,\boldsymbol{b} = \begin{vmatrix}a_1 & a_2\\ b_1 & b_2\end{vmatrix} = a_1b_2-a_2b_1. \tag{11}$$

The deterministic portion of the stochastic Melnikov process is

$$\begin{aligned}M_{\mathrm{d}} &= \int_{-\infty}^{+\infty}\left(\frac{\partial H(x,y)}{\partial y}g_2(x,y,t+t_0)\right.\\ &\quad\left.+\frac{\partial H(x,y)}{\partial x}g_1(x,y,t+t_0)\right)\Big|_{\boldsymbol{\Gamma}(t)}\mathrm{d}t,\end{aligned} \tag{12}$$

and the stochastic portion is

$$M_{\mathrm{s}} = \int_{-\infty}^{+\infty}\frac{\partial H(x,y)}{\partial y}(\xi(t+t_0))|_{\boldsymbol{\Gamma}(t)}\,\mathrm{d}t. \tag{13}$$

The mean of the stochastic Melnikov process $E[M(t_0)]=M_{\mathrm{d}}$ since $E[M_{\mathrm{s}}]=0$. If $\xi(t)$ is considered as an input of Eq. (13), then the impulse response function is

$$h(t) = \frac{\partial H(x,y)}{\partial y}\Big|_{\boldsymbol{\Gamma}(t)},$$

and the corresponding frequency response function is

$$H(\omega) = \int_{-\infty}^{+\infty} h(t)\,\mathrm{e}^{-\mathrm{i}\omega t}\,\mathrm{d}t = \int_{-\infty}^{+\infty} \frac{\partial H(x,y)}{\partial y}\Big|_{\Gamma(t)}\,\mathrm{e}^{-\mathrm{i}\omega t}\,\mathrm{d}t. \quad (14)$$

Thus, the second moment of the stochastic portion can be derived through the convolution integral as a filtering process in the frequency domain as follows:

$$E[M_{\mathrm{s}}^2] = \int_{-\infty}^{+\infty} |H(\omega)|^2 S(\omega)\,\mathrm{d}\omega. \quad (15)$$

From the viewpoint of the Smale–Birkhoff theorem, if the Melnikov function has a simple zero point, the transversal intersection between the stable and unstable manifolds will occur. Once the two manifolds intersect, they will intersect infinite times, indicating the appearance of chaos. However, the mean of the stochastic Melnikov process is usually negative and not zero since the average ignores the effects of stochastic excitations. However, the standard Melnikov method only provides a necessary condition for the occurrence of chaos in the sense of Smale's horseshoes. Accordingly, the criterion for chaotic behavior in stochastic systems can be described with a mean-square representation in view of energy.[5] That is, the stochastic Melnikov process has a simple zero point associated with the mean-square criterion when $M_{\mathrm{d}}^2 = \mu^2 E[M_{\mathrm{s}}^2]$, which yields the threshold for the onset of noise-induced chaos.

As mentioned above, we discuss the possible domain for the onset of chaos in a nonlinear system with two illustrative examples.

3.2. Example 1: Duffing system

Consider the Duffing system as

$$\ddot{x} - x + x^3 = \varepsilon(-\delta\dot{x} + \mu\xi(t)). \quad (16)$$

By variable substitution $y = \dot{x}$, system (16) can be expressed as the equivalent differential equations as follows:

$$\begin{aligned} \dot{x} &= y, \\ \dot{y} &= x - x^3 + \varepsilon(\mu\xi(t) - \delta y). \end{aligned} \quad (17)$$

The Hamiltonian function of the unperturbed system relating to system (17) is

$$H(x,y) = \frac{1}{2}y^2 - \frac{1}{2}x^2 + \frac{1}{4}x^4. \quad (18)$$

We obtain the homoclinic orbits as follows:

$$\Gamma_{\mathrm{hom}}^{\pm}(t) = \left(x^0(t), y^0(t)\right)^{\mathrm{T}} = \pm\left(\sqrt{2}\sec h(t), -\sqrt{2}\sec h(t)\tan h(t)\right)^{\mathrm{T}}. \quad (19)$$

The stochastic Melnikov function for system (17) can be written as

$$M(t_0) = \int_{-\infty}^{+\infty} y^0(t)(\mu\xi(t+t_0) - \delta y^0(t))\,\mathrm{d}t = \mu M_{\mathrm{s}} + M_{\mathrm{d}}, \quad (20)$$

where

$$M_{\mathrm{d}} = -\delta\int_{-\infty}^{+\infty} (y^0(t))^2\,\mathrm{d}t \text{ and } M_{\mathrm{s}} = \int_{-\infty}^{+\infty} y^0(t)\xi(t+t_0)\,\mathrm{d}t.$$

Based on the above derivation, the impulse response function is $h(t) = y^0(t)$, which correlates with the frequency response function as follows:

$$\begin{aligned} H(\omega) &= \int_{-\infty}^{+\infty} y^0(t)\,\mathrm{e}^{-\mathrm{i}\omega t}\,\mathrm{d}t \\ &= \mp\int_{-\infty}^{+\infty} \sqrt{2}\sec h(t)\tan h(t)(\cos\omega t - \mathrm{i}\sin\omega t)\,\mathrm{d}t \\ &= \pm\mathrm{i}\sqrt{2}\int_{-\infty}^{+\infty} \sec h(t)\tan h(t)\sin(\omega t)\,\mathrm{d}t \\ &= \mp\mathrm{i}\sqrt{2}\omega\pi\sec h(\pi\omega/2). \end{aligned} \quad (21)$$

Thus, the second moment of the stochastic part of the Melnikov process can be obtained in the frequency domain as follows:

$$E[M_{\mathrm{s}}^2] = 4q\nu\pi\int_{-\infty}^{+\infty} \sec h^2(\pi\omega/2)\frac{\omega^2}{\omega^2+\nu^2}\,\mathrm{d}\omega. \quad (22)$$

As mentioned above, when $E[\mu^2 M_{\mathrm{s}}^2] = M_{\mathrm{d}}^2$, the threshold of chaos induced by trichotomous noise in system (17) can be expressed as

$$\begin{aligned} \mu &= \frac{\delta\int_{-\infty}^{+\infty}\sec h^2(t)\tan h^2(t)\,\mathrm{d}t}{\sqrt{q\nu\pi\int_{-\infty}^{+\infty}\sec h^2(\pi\omega/2)\dfrac{\omega^2}{\omega^2+\nu^2}\,\mathrm{d}\omega}} \\ &= \frac{\sqrt{\tau}\delta\int_{-\infty}^{+\infty}\sec h^2(t)\tan h^2(t)\,\mathrm{d}t}{\sqrt{q\pi\int_{-\infty}^{+\infty}\sec h^2(\pi\omega/2)\dfrac{\omega^2\tau^2}{1+\omega^2\tau^2}\,\mathrm{d}\omega}}. \end{aligned} \quad (23)$$

3.3. Example 2: Josephson-junction system

We consider the Josephson-junction system perturbed by trichotomous noise excitation as follows:

$$\frac{\mathrm{d}^2\theta}{\mathrm{d}t^2} + \sin\theta + \varepsilon\left[\alpha\frac{\mathrm{d}\theta}{\mathrm{d}t} - \mu\xi(t)\right] = 0. \quad (24)$$

With the transformation $\theta = x$, $\dot{\theta} = y$, system (24) can be changed into the following equivalent form:

$$\begin{aligned} \dot{x} &= y, \\ \dot{y} &= -\sin(x) + \varepsilon(-\alpha y + \mu\xi(t)). \end{aligned} \quad (25)$$

The Hamiltonian function of the unperturbed system associated with system (25) is

$$H(x,y) = y^2/2 + 1 - \cos(x). \quad (26)$$

The analytical solutions of two heteroclinic orbits can be calculated from

$$\Gamma_{\mathrm{het}}^{\pm}(t) = \left(x^1(t), y^1(t)\right)^{\mathrm{T}} = \pm\left(2\arctan(\sinh(t)), 2\sec h(t)\right)^{\mathrm{T}}. \quad (27)$$

In a similar way, we derive the stochastic Melnikov func-

tion of system (25) as

$$M(t_0) = \int_{-\infty}^{+\infty} y^1(t)(-\alpha y^1(t) + \mu\xi(t+t_0))\,\mathrm{d}t = \mu M_\mathrm{s} + M_\mathrm{d}, \tag{28}$$

where

$$M_\mathrm{d} = -\alpha\int_{-\infty}^{+\infty}(y^1(t))^2\,\mathrm{d}t = -8\alpha \text{ and } M_\mathrm{s} = \int_{-\infty}^{+\infty} y^1(t)\xi(t+t_0)\,\mathrm{d}t.$$

As in the case of the Duffing system, the corresponding frequency response function is

$$H(\omega) = \int_{-\infty}^{+\infty} y^1(t)\,\mathrm{e}^{-\mathrm{i}\omega t}\,\mathrm{d}t = \pm 2\int_{-\infty}^{+\infty} \mathrm{sec}\,h(t)\cos(\omega t)\,\mathrm{d}t = \pm 2\pi\,\mathrm{sec}\,h(\pi\omega/2). \tag{29}$$

Thus, the second moment of the stochastic part M_s, as the output of the system in the frequency domain, can be expressed as

$$E[M_\mathrm{s}^2] = 8q\nu\pi\int_{-\infty}^{+\infty}\mathrm{sec}\,h^2(\pi\omega/2)\frac{1}{\omega^2+\nu^2}\,\mathrm{d}\omega. \tag{30}$$

Then, the conditions of occurrence of chaos for the stochastic Melnikov process in system (25) can be obtained in the mean-square sense as

$$M_\mathrm{d}^2 = E[\mu^2 M_\mathrm{s}^2] = \mu^2 E[M_\mathrm{s}^2] = 8q\nu\mu^2\pi\int_{-\infty}^{+\infty}\mathrm{sec}\,h^2(\pi\omega/2)\frac{1}{\omega^2+\nu^2}\,\mathrm{d}\omega. \tag{31}$$

Hence, the threshold for chaotic behaviors in system (25) can be obtained from

$$\mu = \sqrt{\frac{8\alpha^2}{q\nu\pi\int_{-\infty}^{+\infty}\mathrm{sec}\,h^2(\pi\omega/2)\frac{1}{\omega^2+\nu^2}\,\mathrm{d}\omega}} = \sqrt{\frac{8\tau\alpha^2}{q\pi\int_{-\infty}^{+\infty}\mathrm{sec}\,h^2(\pi\omega/2)\frac{\tau^2}{1+\omega^2\tau^2}\,\mathrm{d}\omega}}. \tag{32}$$

Equations (23) and (32) show the condition of the onset of chaos in the Duffing system and the Josephson-junction system, respectively. Without loss of generality, we assume the parameter values $\delta = 0.15, \alpha = 0.1$ for later discussion. The relations between the correlation time τ, probability q and the amplitude threshold μ for the onsets of chaotic behaviors are obtained as depicted in Fig. 3. It indicates straightforwardly that as the correlation τ increases for $q = 0.1, 0.2, 0.3$, and 0.5, respectively, the threshold μ for the occurrence of chaos first decreases rapidly, then increases again slowly for system (16),

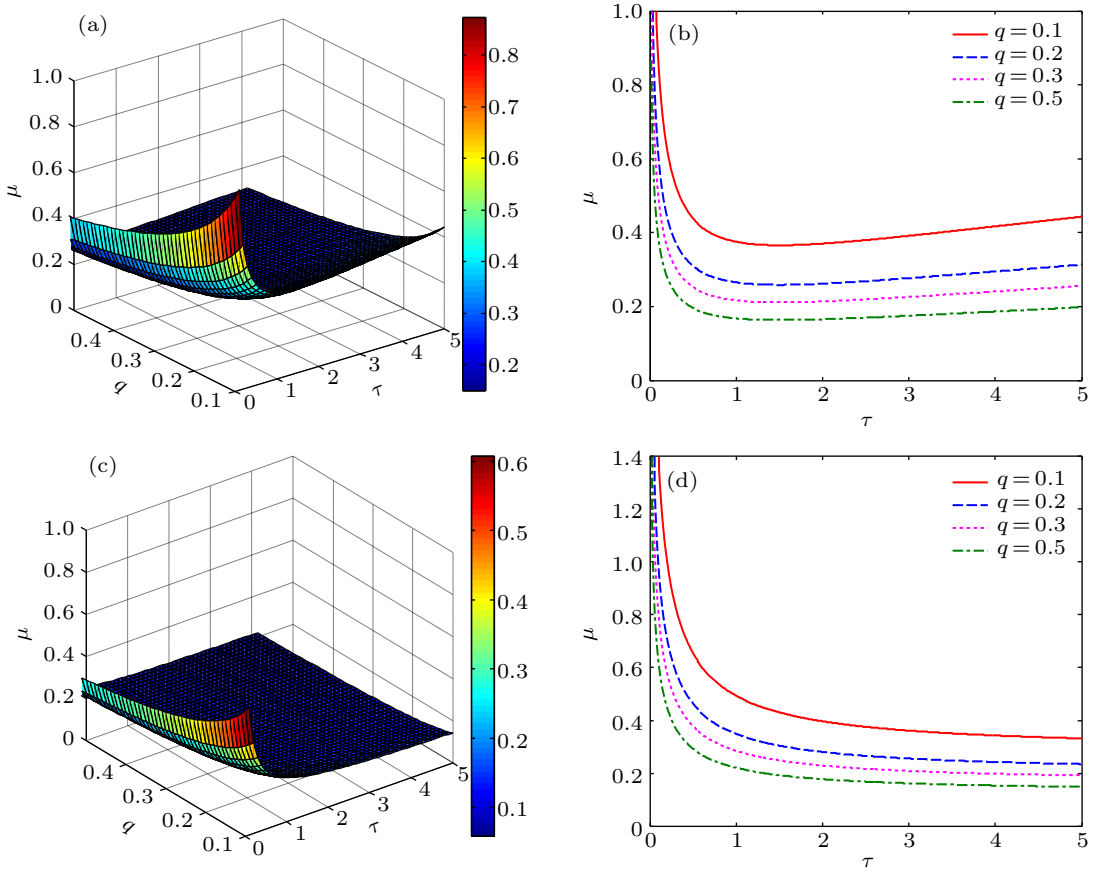


Fig. 3. (color online) Chaotic threshold μ for system (16) ((a), (b)) and system (24) ((c), (d)). Panels (a) and (c) show the analytical results of the relations among τ, q and μ; panels (b) and (d) display the analytical results of the relations between τ and μ for $q = 0.1, 0.2, 0.3$, and 0.5, respectively.

but for system (24) the threshold μ decreases continuously just with the speed from fast to slow. In other words, trichotomous noise can induce different chaotic responses for the two illustrative systems. In the situation where τ is fixed, due to the increase of q, the threshold μ is found to decrease continually for both systems as shown in Figs. 3(b) and 3(d). In particular, while $q = 0.5$, trichotomous noise degrades into dichotomous noise, both of them have similar properties, but trichotomous noise with other stationary probabilities rules out chaos more easily than dichotomous noise since the latter has a smaller chaotic threshold, given the same correlation time. This clearly indicates that one may enhance the threshold of chaos to suppress the occurrence of chaos in the system through properly adjusting the correlation time and the stationary probabilities of trichotomous noise.

4. Numerical methods

Since the result obtained by the stochastic Melnikov method together with the mean-square criterion is not a necessary and sufficient condition for the occurrence of chaos, it is desirable for us to further account for the analytical result by using numerical simulations.

4.1. Mean largest Lyapunov exponent

For the existence of chaos, the system can be judged intuitively from the largest Lyapunov exponent which characterizes the exponential rate of divergence or convergence of nearby orbits. A positive largest Lyapunov exponent means that in phase space of the system, no matter how close the two initial trajectories are, the difference between them will increase exponentially with time evolution so that the long-term behavior of the system cannot be predicted. We utilize Wolf's algorithm[46] to calculate the largest Lyapunov exponent. The basic idea of Wolf's algorithm is to study the long-term evolution of infinitesimal n-dimensional sphere under the initial condition. The Lyapunov exponent is defined as

$$\lambda = \lim_{t\to\infty} \frac{1}{t} \log_2 \frac{p(t)}{p(0)},$$

where $p(t)$ is the length of principal axis of this sphere. Note that the direction of principal axis is always chosen with probability 1 since it cancels out other directions with time evolution. So we can obtain with probability 1 the largest Lyapunov exponent given an arbitrary initial condition and its tangent vector. In the chaotic system, the length evolution in the axis direction is very fast, in order to prevent it from overflowing, we use the Gram–Schmidt orthonormal process. For the largest Lyapunov exponent, we only need to do unitization for each iteration process.

However, for the stochastic system, we can only determine the speed of divergence or convergence of a sample orbit. Thus, in this work for minimizing the effect of random orbits,[47] we utilize the mean largest Lyapunov exponent for investigating whether the system with a stochastic excitation is chaotic through averaging different sample orbits.

For the nonlinear system with given initial value under the trichotomous noise excitation, if an external noise orbit is selected as input, then a sample orbit of the stochastic system will be obtained as output correspondingly, whose processing method can be similar to that of the deterministic system,[48] by using the variation equation to obtain the linearized system along the fiducial sample orbit. The average divergence or convergence degree of sample orbits can be described through the linearized system. Then, we select another sample orbit to repeat the calculation of the largest Lyapunov exponent L_i, where i denotes the serial number of the orbit. Finally, the average of all the largest Lyapunov exponents of the sample orbits is the mean largest Lyapunov exponent, i.e., $L = \frac{1}{N}\sum_{i=1}^{N} L_i$, where N is the number of total orbits. In this work, we choose $N = 100$ for averaging. The plots of the mean largest Lyapunov exponent L versus trichotomous noise amplitude μ for various values of correlation time τ and probability q in systems (16) and (24) are shown in Fig. 4. As seen from Figs. 4(a) and 4(c), the phenomena of the two systems are similar to each other. We vary correlation time τ in a range between 0.1 and 3 and keep $q = 0.3$ fixed, when the amplitude of trichotomous noise μ increases to a critical value (around $\mu_C = 0.67, 0.48, 0.79$, see Fig. 4(a); $\mu_C = 1.35, 0.70, 1.10$, see Fig. 4(c), for $\tau = 0.1, 1, 3$, respectively), the mean largest Lyapunov exponent turns into a positive value from a negative one, signifying the occurrence of chaotic motions. It is also observed from Figs. 4(a) and 4(c) that with increasing correlation time, the critical value first decreases and then increases. Moreover, when we fix the value of μ, such as $\mu = 0.6$ in system (16) and $\mu = 0.9$ in system (24), the dynamical behaviors of both systems will change with the increase of correlation time τ: from non-chaos to chaos (from $\tau = 0.1$ to $\tau = 1$), and then from chaos to non-chaos again (from $\tau = 1$ to $\tau = 3$). This means that chaos in the nonlinear system can be modified and controlled by adjusting the correlation time of trichotomous noise which can not only induce but also suppress the onset of chaos in the system. In Figs. 4(b) and 4(d), correlation time τ is fixed at 1, when the probability q ranges from 0.1 to 0.5, the corresponding mean largest Lyapunov exponent also varies from a negative value to a positive one, but the critical value decreases continually, which shows that trichotomous noise rules out chaos more easily than dichotomous noise when τ is fixed. In addition, in the case of system (24), when $q = 0.1$ and 0.2, we see that the mean largest Lyapunov exponent does not increase continually, but decreases after first increasing with the increase of the amplitude μ.

To better reveal the dependence of the threshold on the correlation time and stationary probability, the plots of func-

tion of the amplitude threshold versus the correlation time for various values of probability are obtained by selecting the critical value of the mean largest Lyapunov exponent (from non-chaos to chaos) as shown in Figs. 5(a)–5(f). On the one hand, if the value of probability q is fixed, then the threshold of amplitude μ for the occurrence of chaos shows the phenomenon of the increase after first reduction with the increase of correlation time τ. On the other hand, for a fixed correlation time, the threshold μ will decrease with the increase of probability q. A comparison between Fig. 3(b) and Fig. 5(a) shows that

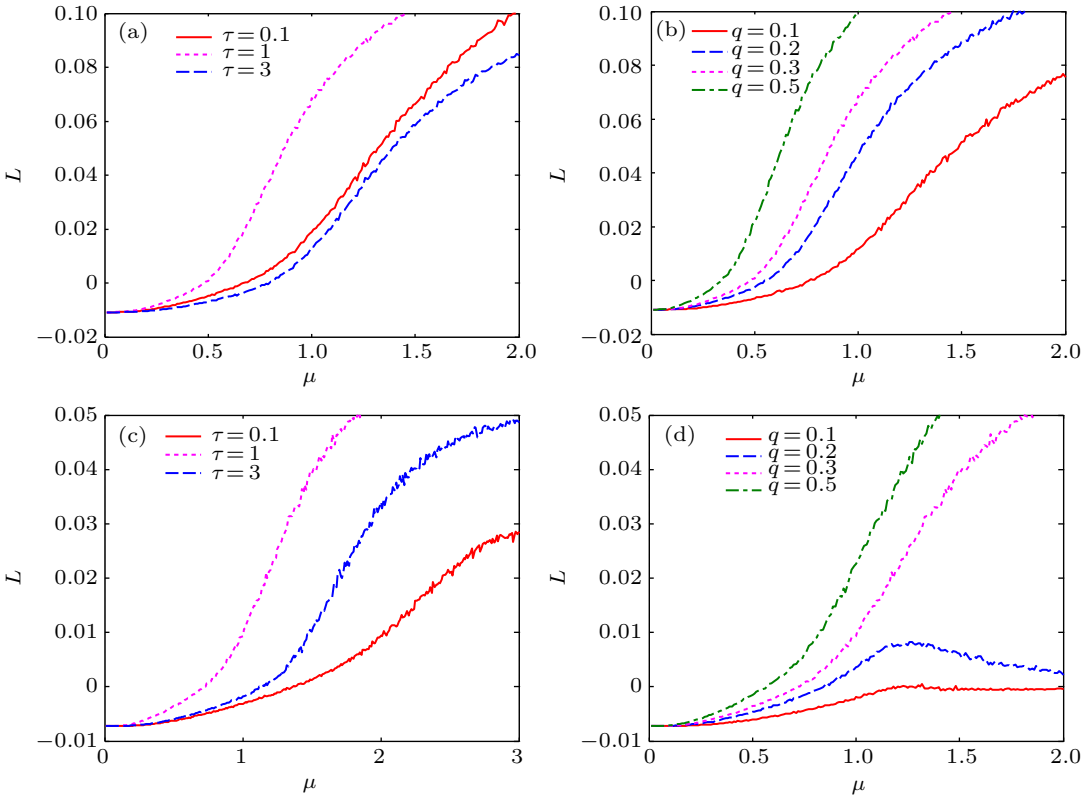


Fig. 4. (color online) Plots of mean largest Lyapunov exponent L versus amplitude μ in system (16) ((a), (b)) and system (24) ((c), (d)) with $q = 0.3$ ((a), (c)), and $\tau = 1$ ((b), (d)).

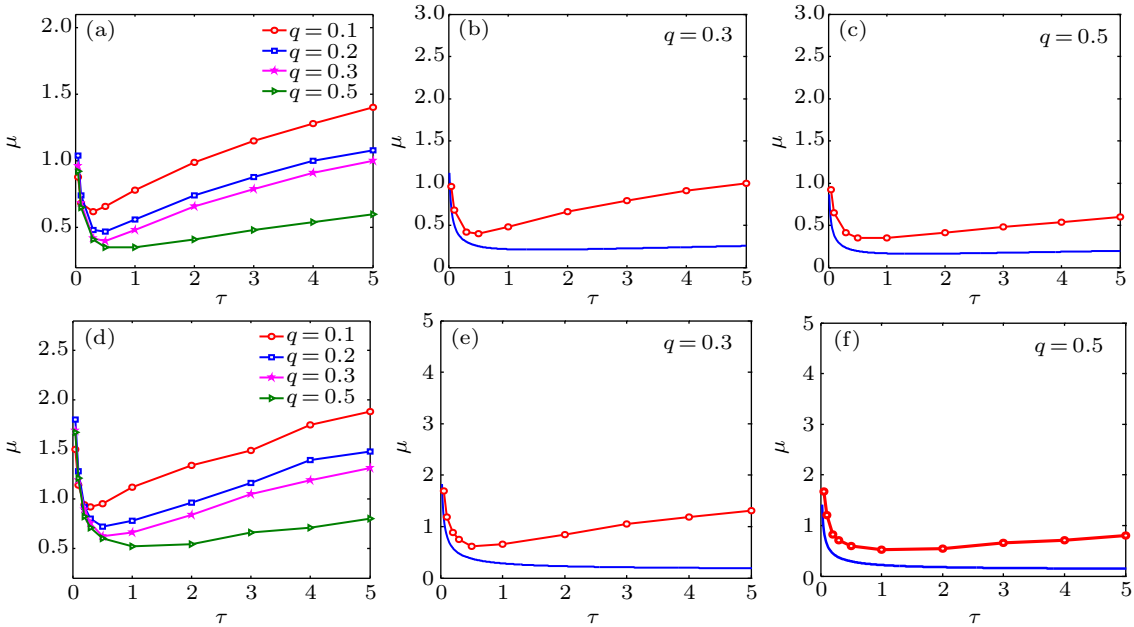


Fig. 5. (color online) Plots of chaotic threshold μ versus correlation time τ for system (16) ((a)–(c)) and system (24) ((d)–(f)). Panels (a) and (d) show numerical results of the relationship between τ and μ for different q values; in panels (b), (c), (e), and (f). '—' denotes analytical result; '··' refers to numerical result.

in system (16), the variation tendency of the analytical results obtained by the stochastic Melnikov method under the mean-square sense is the same as the one of numerical results obtained by selecting the mean largest Lyapunov exponent critical value, but a comparison between Fig. 3(d) and Fig. 5(d) indicates that in system (24), the variation tendency of the former differs from that of the latter. This can be explained since the mean of the stochastic Melnikov process only serves as a necessary condition for the occurrence of chaos. More specifically, it can be seen from Figs. 5(b), 5(c), 5(e), and 5(f) that the smaller the value of τ and the bigger the value of q, the smaller the difference between the analytical and numerical results becomes, for both systems. It follows that the stochastic Melnikov method associated with the mean-square criterion can generate reasonable analytical results for the onset of chaos.

4.2. Phase diagrams and time histories

We utilize phase diagrams and time histories to numerically investigate dynamical behaviors. Figures 6(a)–6(c) exhibit the phase trajectories and time histories of system (16) corresponding to Fig. 4(a) where μ is chosen to be 0.6 and the mean largest Lyapunov exponents are about $-0.002, 0.010$, and -0.005 for $\tau = 0.1, 1$, and 3, respectively. Similarly, figures 6(d)–6(f) exhibit the phase trajectories and time histories of system (24) matching with Fig. 4(c) where we fix $\mu = 0.9$ and the mean largest Lyapunov exponents are about $-0.003, 0.007$, and -0.002, respectively. After taking the two different initial values and getting rid of transient time $t = 10^6$, the trajectories are almost coincident with those shown in Figs.6(a), 6(c), 6(d), and 6(f) in which the mean largest Lyapunov exponents are negative. However, the evolutions of the trajectories are obviously different for the two more closely initial values due to the positive mean largest Lyapunov exponents in Figs. 6(b) and 6(e). These plots elucidate that results of phase diagrams and time histories are in good agreement with the ones of the mean largest Lyapunov exponent, which depicts the sensitive dependence on initial condition in the chaotic system.

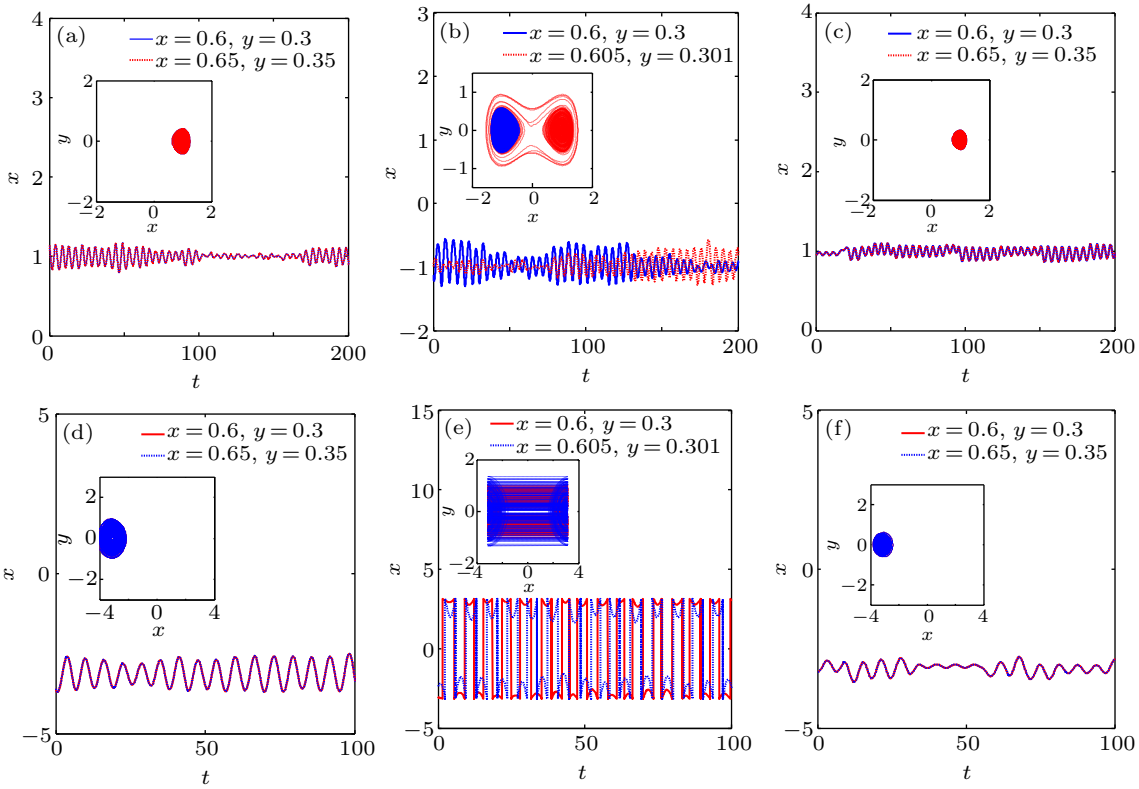


Fig. 6. (color online) Phase diagrams and time histories with $q = 0.3$ for different initial conditions and correlation times in system (16) ((a)–(c)) and system (24) ((d)–(f)), respectively, with ((a), (d)) $\tau = 0.1$, ((b), (e)) $\tau = 1$, and ((c), (f)) $\tau = 3$.

5. Conclusions

In the present paper, the effects of trichotomous noise excitation on the chaotic behaviors of the Duffing system and the Josephson-junction system are discussed, analytically and numerically. The stochastic Melnikov process in the mean-square sense is used to obtain the threshold of trichotomous noise amplitude for the onset of chaos. When the stationary probability of trichotomous noise is fixed and the correlation time increases, the threshold of noise amplitude for the onset of chaos increases after decreasing first in the Duffing system, but always decreases continuously in the Josephson-junction system. However, in reverse, with the increasing of the sta-

tionary probability of trichotomous noise whose correlation time is fixed, the threshold decreases continually in both systems. The extensive numerical simulations including the mean largest Lyapunov exponent, phase diagrams and time histories are carried out to verify the analytical results, and we can see that both results are in agreement with each other. We conclude that the correlation time and the stationary probability of trichotomous noise play significant roles in inducing and suppressing chaos in both the Duffing system and the Josephson-junction system.

References

[1] Koch B P and Leven R W 1985 *Physica D* **16** 1
[2] Ariaratnam S T, Xie W C and Vrscay E R 1989 *Dyn. Stability Syst.* **4** 111
[3] Shaw S W and Rand R H 1989 *Inter. J. Non-Linear Mech.* **24** 41
[4] Xie W C 1994 *Nonlinear Stochastic Dynamics, AMD* **192** 215
[5] Lin H and Yim S C S 1996 *ASME J. Appl. Mech.* **63** 509
[6] Awrejcewicz J and Sendkowski D 2004 *Phys. Lett. A* **330** 371
[7] Awrejcewicz J and Pyryev Y 2006 *Nonlinear Anal., Real World Appl.* **7** 12
[8] Awrejcewicz J and Holicke M 2006 *Math. Probl. Eng.* **2006** 1
[9] Lei Y M and Xu W 2007 *Acta Phys. Sin.* **56** 5103 (in Chinese)
[10] Zhang W, Yao M H and Zhang J H 2009 *J. Sound Vib.* **319** 541
[11] Yang X W, Tian R L, Cao Q J and Wu Q L 2012 *Chin. Phys. B* **21** 20503
[12] Elston T C and Doering C R 1996 *J. Stat. Phys.* **83** 359
[13] Horsthemke W and Lefever R 1984 *Noise-induced Transitions* (Berlin: Springer)
[14] Bena I, Van den Broeck C, Kawai R and Lindenberg K 2002 *Phys. Rev. E* **66** 045603
[15] Gitterman M 2003 *Phys. Rev. E* **67** 057103
[16] Li J H and Han Y X 2006 *Phys. Rev. E* **74** 051115
[17] Lei Y M, Fu R, Yang Y and Wang Y Y 2016 *J. Sound Vib.* **363** 68
[18] Li P, Nie L R, Lü X M and Zhang Q B 2011 *Chin. Phys. B* **20** 100502
[19] Mankin R, Ainsaar A and Reiter E 2000 *Phys. Rev. E* **61** 6359
[20] Mankin R, Ainsaar A and Reiter E 1999 *Phys. Rev. E* **60** 1374
[21] Mankin R, Laas K, Laas T and Reiter E 2008 *Phys. Rev. E* **78** 031120
[22] Laas K, Mankin R and Rekker A 2009 *Phys. Rev. E* **79** 051128
[23] Gitterman M 2012 *Physica A* **391** 5343
[24] Mankin R, Soika E and Lumi N 2014 *Physica A* **411** 128
[25] Mankin R, Ainsaar A, Haljas A and Reiter E 2002 *Phys. Rev. E* **65** 051108
[26] Mankin R, Soika E and Sauga A 2008 *WSEAS Trans. Syst.* **7** 239
[27] Soika E, Mankin R and Priimets J 2012 *Proc. Est. Acad. Sci., Phys. Math.* **61** 113
[28] Guo F, Li H and Liu J 2014 *Physica A* **409** 1
[29] Soika E and Mankin R 2010 *WSEAS Trans. Biol. Biomed.* **7** 21
[30] Zhong S C, Wei K, Gao S L and Ma H 2015 *J. Stat. Phys.* **159** 195
[31] Lin L F, Chen C and Wang H Q 2016 *J. Stat. Mech.* **2016** 023201
[32] Yang T T, Zhang H Q, Xu Y and Xu W 2014 *Inter. J. Non-Linear Mech.* **67** 42
[33] Zhang H Q, Yang T T, Xu Y and Xu W 2015 *Eur. Phys. J. B* **88** 1
[34] Birx D L and Pipenberg S J 1992 *IEEE International Joint Conference on Neural Network*, June 7–11, 1992, p. 881
[35] Frey M and Simiu E 1993 *Physica D* **63** 321
[36] Privault N 1994 *Stochastics, Stochastics Rep.* **51** 83
[37] Kendall B 2001 *Chaos, Solitons & Fractals* **12** 321
[38] Cveticanin L and Zukovic M 2009 *J. Sound Vib.* **326** 768
[39] Sharma A, Patidar V, Purohit G and Sud K K 2012 *Commun. Nonlinear Sci. Numer. Simul.* **17** 2254
[40] Srinil N and Zanganeh H 2012 *Ocean Eng.* **53** 83
[41] Li Y, Yuan Y, Mandic D P and Yang B J 2009 *Chin. Phys. B* **18** 958
[42] Likharev K K and Semenov V K 1991 *IEEE Trans. Appl. Supercond.* **1** 3
[43] Makhlin Y, Schön G and Shnirman A 2001 *Rev. Mod. Phys.* **73** 357
[44] Wang J S, Liang B L and Fan H Y 2008 *Chin. Phys. B* **17** 697
[45] Wiggins S 1988 *SIAM J. Appl. Math.* **48** 262
[46] Wolf A, Swift J B, Swinney H L and Vastano J A 1985 *Physica D* **16** 285
[47] Sano M and Sawada Y 1985 *Phys. Rev. Lett.* **55** 1082
[48] He T and Habib S 2013 *Chaos* **23** 033123